# Quantum Dynamics of the Eley−Rideal Hydrogen Formation Reaction on Graphite at Typical Interstellar Cloud Conditions†

**Simone Casolo,‡ Rocco Martinazzo,*,‡,§ Matteo Bonfanti,‡ and Gian Franco Tantardini‡,§,||**

*Dipartimento di Chimica Fisica ed Elettrochimica, Università degli Studi di Milano, V. Golgi 19, 20133 Milan, Italy; CIMAINA, Interdisciplinary Center of Nanostructured Materials and Interfaces, University of Milan; and CNR Institute of Molecular Sciences and Technology, V. Golgi 19, 20133 Milan, Italy*

*Received: April 30, 2009*

Eley−Rideal formation of hydrogen molecules on graphite, as well as competing collision induced processes, are investigated quantum dynamically at typical interstellar cloud conditions, focusing in particular on gas-phase temperatures below 100 K, where much of the chemistry of the so-called diffuse clouds takes place on the surface of bare carbonaceous dust grains. Collisions of gas-phase hydrogen atoms with both chemisorbed and physisorbed species are considered using available potential energy surfaces (Sha et al., *J. Chem. Phys.***2002** *116*, 7158), and state-to-state, energy-resolved cross sections are computed for a number of initial vibrational states of the hydrogen atoms bound to the surface. Results show that (i) product molecules are internally hot in both cases, with vibrational distributions sharply peaked around few (one or two) vibrational levels, and (ii) cross sections for chemisorbed species are 2−3× smaller than those for physisorbed ones. In particular, we find that $H_2$ formation cross sections out of chemically bound species decrease steadily when the temperature drops below ∼1000 K, and this is likely due to a quantum reflection phenomenon. This suggests that such Eley−Rideal reaction is all but efficient in the relevant gas-phase temperature range, even when gas-phase H atoms happen to chemisorb barrierless to the surface as observed, e.g., for forming so-called para dimers. Comparison with results from classical trajectory calculations highlights the need of a quantum description of the dynamics in the astrophysically relevant energy range, whereas preliminary results of an extensive first-principles investigation of the reaction energetics reveal the importance of the adopted substrate model.

## I. Introduction

In recent years, there has been an increased interest in studying hydrogen recombination on graphitic surfaces. This interest is largely due to the relevance of hydrogen−graphite systems for understanding hydrogen formation in the interstellar medium (ISM). Molecular hydrogen is the most abundant molecule in several interstellar structures, ranging from dense to diffuse clouds, from photon-dominated regions to regions with shocked gases, despite the fact that hydrogen molecules are continuously dissociated by stellar UV radiation and cosmic rays. It is now generally accepted that such efficient hydrogen formation can only occur on the surface of interstellar dust grains,[1−3] an ensemble of very small particles of different sizes and nature. In diffuse clouds, where the intense stellar radiation heats the gas, the largest particles are composed of a silicate core covered by an "organic refractory" mantle, while smaller particles are entirely carbonaceous, being even simple polycyclic aromatic hydrocarbons.[4−6] Hydrogen formation in these regions of interstellar space may thus occur on graphitic surfaces, and hydrogen−graphite has become the prototypical system for studying hydrogen formation in the ISM. Depending on the physical conditions of interest and on the actual morphology of the surface, a number of formation processes are possible, and only an accurate knowledge of adsorption, diffusion, and recombinative elementary acts allows one to ascertain with confidence the role of each given pathway, and to estimate the corresponding rate constant.

Hydrogen atoms may adsorb on graphitic surfaces either chemically or physically. Several experimental[7−10] and theoretical[11−15] studies agree on the fact that hydrogen chemisorption on the regular (0001) surface occurs on top of a carbon atom and requires substantial lattice reconstruction, with the carbon atom moving out of the surface plane by about 0.4 due to rehybridization of its valence orbitals. As a consequence, a barrier to chemisorption ∼0.15 eV (∼ 1700 K) high appears, and essentially prevents (direct) hydrogen sticking in the chemisorption well at temperatures typical of the ISM ($T$ = 10−100 K in diffuse clouds).

Hydrogen chemisorption may occur in photon-dominated and shocked regions where the temperature is high enough ($T$ = 500−5000 K) to allow H atoms to overcome the adsorption barrier. Under these conditions, *clustering* of hydrogen atoms occurs at all but very low (<1%) coverages[16−19] as a consequence of the aromatic nature of graphite.[20] In particular, molecular formation at these high temperatures may follow recombination of hydrogen pairs in *para* position of an hexagonal ring,[16] and direct (Eley−Rideal) abstraction may occur on isolated atoms as well as dimers.[21] Langmuir−Hinshelwood reactions, however, are prevented by the lack of mobility of H atoms chemically bound to the surface. In principle, chemisorbed hydrogen atoms can act as catalysts even at low temperature, e.g. via the barrierless adsorption of H atoms at their *para* position, followed by direct Eley−Rideal recombination of the latter.[17,21]

† Part of the "Vincenzo Aquilanti Festschrift".

* To whom correspondence should be addressed. E-mail: rocco.martinazzo@unimi.it.

‡ Dipartimento di Chimica Fisica ed Elettrochimica, Università degli Studi di Milano.

§ CIMAINA, Interdisciplinary Center of Nanostructured Materials and Interfaces, University of Milan.

|| CNR Institute of Molecular Sciences and Technology.

10.1021/jp9040265 
Published on Web 06/11/2009

Physisorbed species are limited by desorption ($T_{des} \approx 30-40$ K) only, and may form hydrogen molecules either through a Langmuir−Hinshelwood, or an Eley−Rideal, or a hot-atom mechanism, or a combination of them. Langmuir−Hinshelwood recombination between neighboring atoms has been shown to be efficient,[22−24] and tunneling guarantees very high mobility of H atoms down to vanishing temperatures.[25]

In this work, we focus on the $H_2$-forming, Eley−Rideal reactions at "cold" energies (i.e., down to 0.1 K) involving either a chemisorbed or a physisorbed atom. Both of them are strongly exothermic ($\Delta E_0 \gtrsim 3.7$ eV), and may in principle proceed at vanishing collision energy. In particular, the adopted interaction potential (see below) does *not* take into account the possible presence of a tiny barrier in the reaction from chemisorbed atoms ($E_{barr} \approx 100$ K according to refs 28 and 43). This is reasonable, as the existence of such a barrier has been inferred so far from density functional theory (DFT) results only, and these are not accurate enough to this end.

Furthermore, we gather insights in the formation of adsorbate-induced trapped (physisorbed) species, i.e., those atoms which get trapped to the surface because of a collision with an adsorbate. These species could possibly contribute to $H_2$ production through collisions with further chemisorbed/physisorbed atoms, potentially at large distances.

As we show in Section II, we find that reactive collisions at low temperature are $2-3\times$ more probable if they involve *physisorbed* H atoms. This result is likely due to the effect of quantum reflection from strong, short-range potentials which—for chemisorbed species—manifests itself at ∼100 K and below. Thus, even though we treat here a simplified model for the collision process of a gas-phase H atom with a second, isolated H atom chemisorbed on the surface, this result reasonably holds also for H atoms being part of a cluster.

The quantum dynamical calculations have been performed with a novel wavepacket approach (see Section II) which, with the help of Fourier mapping and high-quality absorbing-potential techniques, allows us to overcome known problems in studying a collisional dynamics in such cold collision energy regime by means of time-dependent techniques. The method is applied to solve exactly a known reduced-dimensional dynamical model which does *not* take into account the lattice motion. This approximation could be rather severe as a carbon atom has to relax toward the surface plane when the product molecule forms, but it is necessary if one wants to keep the dynamical description at the expensive (but exact) quantum level.

The need of a quantum description in the relevant collision energy range is highlighted in Section III, where we study the same dynamical model by (quasi) classical techniques. Furthermore, the effect of the substrate description (either "adiabatic" or "diabatic") in the reaction involving chemisorbed species is considered. In the same Section, we use *first-principles* electronic structure means on two prototypical substrate models—i.e., the (periodic) graphitic model underlying the potential energy surfaces (PESs) adopted here and the widely used coronene molecule- to investigate the energetics of the same reaction. We find that the substrate model modifies the shape of the potential energy surface in the entrance channel, and this in turn profoundly affects the global dynamical behavior and the reaction probabilities in a rather large energy range. This suggests that currently available models, including dynamically the graphitic lattice but otherwise based on cluster calculations, might need considerable improvement if the aim is to describe Eley−Rideal reactions on graphite.

Overall, our results suggest sizable differences in the Eley−Rideal dynamical behavior of chemisorbed and physisorbed H atoms at typical interstellar cloud conditions. The latter have larger reaction cross sections and, furthermore, show a net tendency to form (translationally) "hot" trapped species, which might contribute to $H_2$ formation. If we also take into account the (tight) kinetic constraints in chemisorbing H atoms,[20] then we are tempted to conclude that hydrogen formation in diffuse clouds either involves physisorbed species only (and *surface* temperature small enough to let them be stable) or cannot be explained by a simple graphitic model. It remains to be established whether including the surface motion would alter substantially these conclusions, but this is all but an easy task as a fully quantum description is presently impracticable and simplified dynamical schemes are of doubt validity in such deep quantum regime.

## II. Calculations and Results

In this work, quantum scattering calculations have been performed within the rigid, flat-surface approximation developed by Persson and Jackson,[26] following the approach of Jackson and Lemoine.[27] In this approximation, the many-body dynamics is reduced to a three-dimensional one involving the coordinates of the two atoms above the surface left out by conservation of the in-plane linear momentum and of the angular momentum along the surface normal. The model thus allows a lateral displacement of the two reacting atoms, which is unphysical when one of them is chemically bound to the surface, and completely neglects the dynamical role of the lattice, both "active" (i.e., when it induces modification in the reaction pathway) and "passive" (i.e., when it acts as a phonon bath). However, as the reaction we are interested in is governed by the entrance channel potential, molecule formation occurs early in the collision process, thereby suggesting that the lateral freedom of the target atom has little effects in forming the reaction products. Furthermore, the active role of the surface is relevant for chemisorbed H atoms only and can be incorporated in the potential energy surface by considering two extreme situations:[28] in the first, "adiabatic" case the carbon atom involved in the bond relaxes instantaneously at each hydrogen atom's position and ends up in the equilibrium position when the molecule leaves the surface; in the second, "diabatic" case hydrogen formation is supposed to occur so fast that the same carbon atom remains fixed at its puckered position up to molecule formation, thereby transferring de facto part of the reaction exothermicity into the phonon bath. Finally, establishing the role of the surface as a heat bath when light atoms are involved is still an open question in surface science, though it might be solved in the near future. In our case, one could make use of a mixed quantum-classical description (H and surface atoms being the quantum and classical systems, respectively) but the low surface temperatures relevant for the ISM chemistry makes this approach equally questionable as the rigid surface approximation. Several previous works dealt with one or more of the above topics, and will be discussed in Section III.

Within the above approximations, both "product" and "reagent" coordinate sets can be used efficiently in a grid-based time-dependent wave packet dynamics, the choice depending on the state-to-state information one is interested in. We already exploited such a possibility in performing a *full* state-to-state analysis of the dynamics at high energies, including the calculation of the total collision-induced-desorption cross section.[29−31] In order to treat the low energy collision regime, we use here essentially the same, *time-dependent* approach

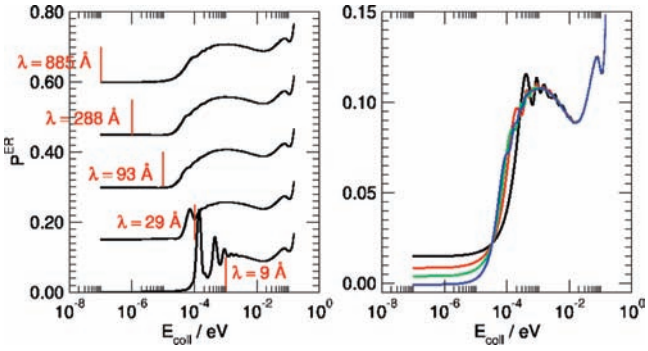


**Figure 1.** Results of tests calculations on the collinear reaction dynamics with a target atom initially in the $v = 0$ vibrational state of the chemisorption well. Left panel: total reaction probability for different values of the strength ($E_{min}$, vertical bars in the graphs) of the transmission-free AP used in the entrance channel, as obtained from 100 ps long wavepacket propagations. Also indicated is the corresponding length, $\lambda$. Right panel: same results as in the left panel, for $E_{min} = 10^{-4}$ eV and different propagation times $T_f$. Black, red, green, and blue curves for $T_f = 10$, 20, 30, and 50 ps, respectively.

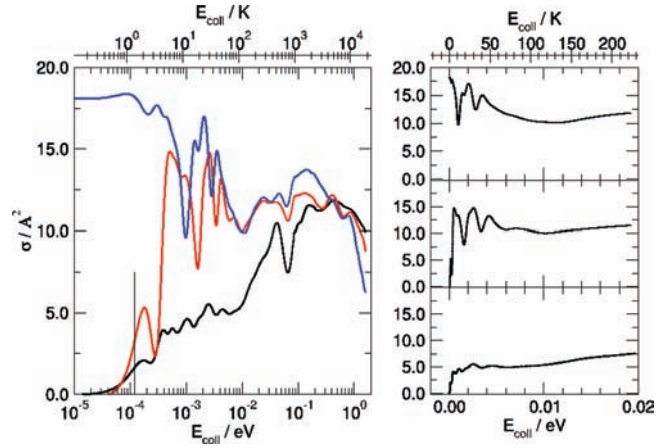


**Figure 2.** Total Eley−Rideal reaction cross sections for chemisorbed species, as functions of the collision energy. Left panel: results on a logarithmic scale with black, red, and blue curves for target atoms initially in the $v = 0$, 1, and 2 vibrational state, respectively. Vertical bar marks the strength of the absorbing potential in the entrance channel. Right panels: from bottom to top for $v = 0$, 1, and 2.

described in ref 30. The main reason for studying this low energy dynamics in the time domain is that such an approach might offer in the near future the unique advantage of including the effect of dissipation, e.g., by exact[32−34] or approximate[34] wave packet techniques.

Technical problems such as the need of large, well-behaving absorbing potentials (APs) have been alleviated with the help of transmission-free absorbing potentials[36] and Fourier-mapping techniques[37] in the reagent coordinate set. The first are specially designed absorbing potentials which essentially remove transmission, thereby allowing one to focus on the reflection problem only. They indeed have one arbitrary parameter only, the strength $E_{min}$ which also sets their length $\lambda = h/\sqrt{2\bar{m}E_{min}}$ ($m$ being the reduced mass of the relevant arrangement and $h$ the Planck's constant) as the longer de Broglie wavelength for which the reflection probability is below 1%. Fourier mapping techniques, on the other hand, allow one to accommodate large absorbing potential regions while keeping the advantage of Fourier pseudospectral techniques. For example, in typical calculations APs as large as 30 Å(corresponding to $E_{min} \approx 10^{-4}$ eV) have been accommodated with less than 300 (mapped) grid points.

One basic problem of the cold collision energy regime, namely the purely *incoming* asymptotic condition in traditional, initial state-selected dynamics, has been recently solved with a *two*-wave packet technique which exploits linearity of the Schrödinger equation.[38] This problem forces one to use large enough initial wavepackets (in coordinate space) to avoid the presence of *outgoing* momentum components which would invalid the traditional time-energy mapping. At the same time, this would result in such a narrow useful energy range to make useless a wave packet approach. Our approach[38] completely removes this problem and allows one to use initial wavepackets zero-momentum centered and arbitrarily narrow in coordinate space, at the expense of propagating *two* (linearly independent) wavepackets in place of one. Details of the theory and its implementation will be given in a forthcoming paper. Here it is sufficient to say that, in order to get accurate results, particular attention has been paid to the convergence properties with respect to the total propagation time and to the length of the absorbing potential. For an example see Figure 1, where we report results of 2D test calculations under quite stringent conditions.

The *first-principles* potential energy surfaces computed and fitted by Sha et al.[28] have been used throughout. In the case of a chemisorbed atom the adopted potential treats adiabatically the motion of the carbon atom involved in the reaction, while the incoming H atom only feels a physisorbed interaction (apart, of course, from the H−H interaction). Both these approximations are quite realistic at low energy, even when the possibility of dimer formation is taken into account. Indeed, low-energy H atom projectiles can hardly overcome the barrier to chemisorption, and are thus confined to the physisorption tail of the interaction potential. The only exception is the para dimer mentioned in Section I, whose formation is truly barrierless. If this possibility is taken into account, then the computed reaction cross sections can (at worse) be considered reasonable *upper* bounds to the true ones. A comparison with results obtained in the diabatic approximation will be performed in the next Section.

Results for the $H_2$ formation cross sections at normal incidence from chemisorbed species are reported in Figure 2, for different values of the vibrational quantum number of the target atom, $v = 0-2$. Only the ground-state data are relevant for the chemistry of diffuse clouds, the excitation energy for $v = 1$ being already too high at typical cloud temperatures; the only reason why we considered this vibrational excitation is that it helps to get insights into the reaction dynamics. In these calculations, wavepacket dynamics has been followed for rather long time (25−30 ps but in same cases up to 80 ps), and a reasonably large absorbing potential has been used in the entrance channel, with strength $E_{min} \approx 10^{-4}$ eV. It is evident from Figure 2 that, with the exception of highest initial vibrationally excited species considered, the computed cross sections decrease steadily as the collision energy drops below ~1000 K. This is likely due to the strong, short-range interaction potential between the two hydrogen atoms which prevents low energy projectiles to enter the exit channel if the corresponding de Broglie wavelength is larger than the range of the potential. This is supported by the fact that the relevant wavelength for H atoms impinging at $10^{-2}$ eV (~3 Å) is already on the order of the range of the H−H potential. Furthermore, collinear test calculations (here not reported) using an artificially cut H−H potential show that the onset of this behavior shifts monotonically at higher energies as the cutoff distance is decreased.

A closer look at the reaction dynamics can be obtained by looking at the rovibrational distributions of the product $H_2$

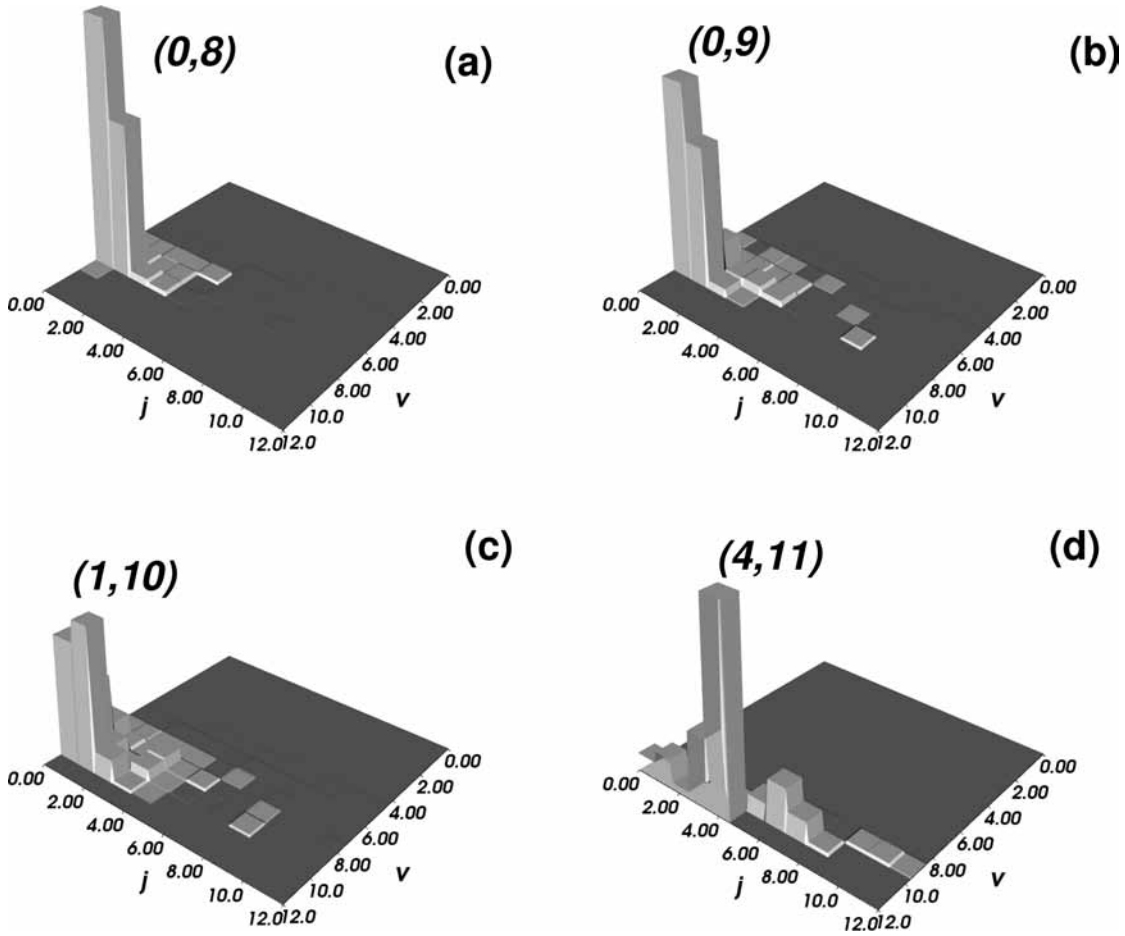


**Figure 3.** Rovibrational distributions of product $H_2$ molecules formed at a collision energy of $10^{-3}$ eV, with the most probable $(j,v)$ values indicated. Panels (a)−(c) for chemisorbed target species with $v = 0-2$, respectively. Panel (d) for an initially physisorbed H atom in its ground vibrational state.

molecules, as reported in Figure 3 at $10^{-3}$ eV collision energy. These results are unchanged for lower energies. The figure reveals that the reaction dynamics proceeds almost collinearly (the resulting rotational angular momentum $j$ is quite small, $j \approx 0 - 1$) and in a vibrationally adiabatic way, i.e., with product vibrational distributions peaking at $v' = 8$, 9, and 10 for targets initially in the $v = 0$, 1, and 2 states, respectively. These values are close to the highest possible, and product molecules leave the surface with only a small fraction of reaction exoergicity released as translational energy ($E_T \approx 0.4 - 0.3$ eV for $v = 0-2$). In addition, the widths of the rovibrational distributions increase as the target atoms are vibrationally more excited, with larger fraction of product molecules appearing with vibrational quantum numbers lower than their most probable value. This suggests that some vibrational relaxation occurs in the entrance channel, thereby allowing the projectile to get rid of quantum reflection when $v > 1$, at least in the energy regime considered here. At lower energies, cross sections are expected to decrease linearly with the speed $v$ of the projectile, in agreement with Wigner's law which predicts a linearly vanishing *probability* for any exoergic process. The difference with the celebrated gas-phase result of a diverging cross section ($\sigma \propto 1/v$) comes from the cross-sectional factor ($\propto 1/v^2$) which converts probabilities to cross sections when a projectile scatters off a center of forces, and which is lacking when the projectile scatters off a *plane* of forces.

Interestingly, the cross sections of Figure 2 show a number of low-energy resonances. Although we cannot rule out traditional Feshbach resonances where part of the energy in the scattering coordinate is temporarily stored in internal degrees of freedom, we notice that some sort of resonance appears even in *one*-dimensional scattering problems when the reflecting well is deep enough to support some bound states.[39] If this were the case, then the corresponding metastable states would live long enough to allow the energy to flow from the projectile translational coordinate (where reflection occurs) to the $H_2$ center-of-mass coordinate, as a consequence of the bouncing with the surface.

The results for Eley−Rideal cross sections from physisorbed species, obtained with similar grid/propagation parameters as mentioned in the previous case, are shown in Figure 4. They are only qualitatively similar to those shown in Figure 2 and, in particular, they start to decrease only (much) below $E_{coll} = 10^{-4}$ eV, where our results could be not well converged because of both the propagation time and the AP length. However, in the astrophysically relevant energy range $E_{coll} = 10^{-2}-10^{-4}$ eV, they are quite large, considerably larger than those previously found at higher energies,[28,31] with peaks $\sim$20 Å$^2$ high. The essential difference with the previous chemisorbed case is the larger *mobility* of the target atom allowed by the physisorption potential: when the projectile gets closer to the adsorbate, the latter has room to rearrange in such a way to increase the effective range of the H−H potential and to shift the onset of the quantum reflection to lower energies. This leads to some rotational excitation of the product molecules [see Figure 3, panel (d)] which, consistently with the large values of the reaction cross section, suggests that noncollinear collisions play an important role in this case. Furthermore, formation of trapped

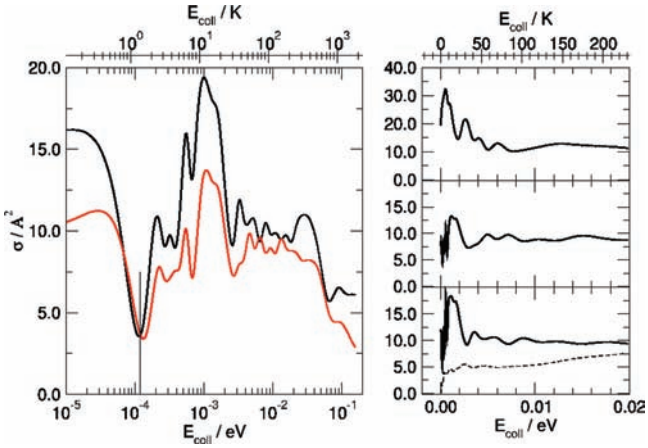


**Figure 4.** Total Eley−Rideal reaction cross sections for physisorbed species, as functions of the collision energy. Left panel: black and red curves for target atoms initially in the $v = 0$ and 1 vibrational state. Vertical bar marks the strength of the absorbing potential in the entrance channel. Right panels: ER cross sections for $v = 0-1$ in the two bottom panels, trapping cross section for $v = 0$ in the top panel. Also reported the results for a chemisorbed atom ($v = 0$) as dashed line in the lower right panel.

species is greatly enhanced when the gas-phase H atom scatters off a physisorbed species, and cross sections as large as ∼30 Å$^2$ are found for forming two atoms bound to the surface, moving parallelly to it (see Figure 4, top right panel). These species might be important at nonzero coverage conditions, since they may recombine with further adsorbed H atoms far away from the site where they formed, and introduce subtle effects in the observed "apparent" reaction cross sections. Indeed, the cross sections would then depend on the coverage and, in addition, on those parameters affecting the mobility (life) of these species trapped on the surface, e.g. the surface temperature.

Before concluding this Section, it is worth noticing that the cross sections reported in Figures 2 and 4 have not been corrected for the electronic spin factor (1/4 for unpolarized H atom beams). When the reaction involves a chemisorbed species this is a subtle effect, as such a correction factor does *not* appear when different substrates (e.g., metals) are considered. Indeed, unlike with metals, when the hydrogen atom is initially chemisorbed on the graphitic surface, the unpaired spin is *not* quenched into the substrate, but rather is accommodated in a *quasi*-localized state close to the adsorbate.[20] Thus, the second (projectile) hydrogen atom has only 1/4 of chance of being in the overall singlet state needed for $H_2$ formation to occur. Note also that the corrected trapping cross sections are expected to be similar to or larger than those shown in Figure 4 (top right panel) as trapping can occur both in the singlet and in the triplet state (though in the latter case it would profit of the absence of any reactive competing channel).

## III. Discussion

As many previous studies dealt with the Eley−Rideal hydrogen recombination on graphite,[12,22,28−31,40−50] in this Section we analyze our results in deeper detail by critically examining both the approximations introduced and the results of similar studies available in the literature. We only focus on the reaction involving chemisorbed H atoms, as this has been subjected to intense research activity in search of reaction pathways involving stable species and able to explain hydrogen formation at ISM conditions. The reason for this Section, of course, is that none of these studies (including the present one) can give definitive answers to such an astrophysically important question, and we hope in this way to help the reader to save the message(s) from this and related works.

**A. Classical vs Quantum Dynamics.** As the range of validity of classical mechanics in exoergic, barrierless reactions might not be obvious, we begin with showing the results of a quasi-classical dynamical study performed on exactly the same potential energy surface used in the quantum calculations outlined in Section II. "Quasi" means that quantization of the target vibrational motion is handled by properly sampling the initial conditions of the classical trajectories in such a way to reproduce the classical phase space density corresponding to the relevant quantum level. Classical calculations have been performed using standard techniques and were detailed in our previous paper,[30] the only difference is that now special care has been devoted to the choice of the propagation time, as quite low collision energies are involved. Results are shown in Figure 5, along with the results of Figure 2 for comparison. As is evident from the figure, classical mechanics does a pretty good job in reproducing the cross section at high energies (apart from undulations not visible on the logarithmic scale used in the graph and already discussed in our recent works),[29,30] but fails, as expected, in reproducing both the low energy resonances and the correct low energy behavior. In particular, classical cross sections start to diverge considerably from the quantum ones in the astrophysically relevant energy range $T < 100$ K and have a wrong limiting behavior, tending toward nonzero values. This behavior parallels known, marked differences between the classical and the quantum description of the sticking of atoms to surfaces. It is worth noticing at this point that the potential energy surface used is truly barrierless, that is, the observed differences do not arise from simple tunneling phenomena, rather they are entirely due to the effect of particle vs wave propagation in a classically allowed region (quantum reflection). It follows that, even *without* a reaction barrier, classical studies of the title reaction have a limited value in the astrophysically relevant energy range.

**B. Adiabatic vs Diabatic Models.** As in Section II, we considered, for H chemisorbed species, only one of the two possible limiting ways to implicitly include the important carbon atom in the dynamical model, we focus here on the case of a (substrate) diabatic dynamics. Only the case of a target initially in its ground vibrational state is considered, the results for $v > 0$ being very similar. Results of these quantum calculations with the diabatic potential energy surface developed by Sha et al.[28] are shown in Figure 6 where it is clear that, apart from a difference in magnitude ≲4 Å$^2$ over the whole energy range, the cross-section behavior is very similar in the two cases. This suggests that the same is true when including dynamically the carbon atom motion, and then that our general conclusion on the low energy behavior of the Eley−Rideal cross section should not be affected by a more exact treatment of the reaction dynamics. There are, of course, expected differences in the reaction energy partitioning as the way the carbon atom relaxes toward the (bare) surface equilibrium position determines both the amount of energy left to the substrate and the energy going to internal excitation of the product molecules. We only note here that, even with the above two rigid-surface models, there are quantitative differences in the vibrational excitation of the $H_2$ molecules. However, we do not attempt to compare these results with experimentally measured rovibrational distributions as the description of the $H_2$ potential energy curve of the adopted PES (analogously to many others in the literature) differs substantially from the exact one. Finally, it is not obvious that

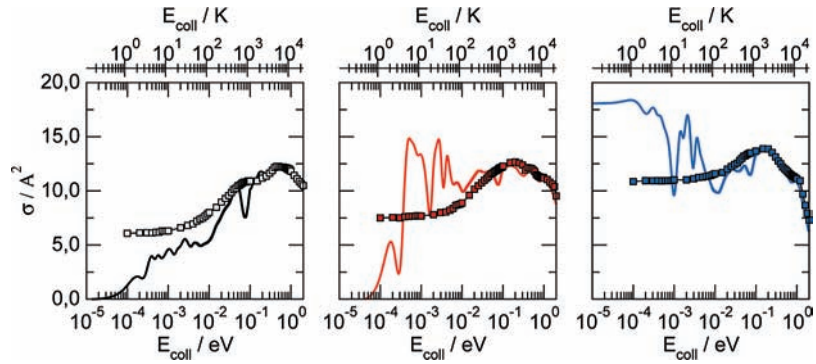


**Figure 5.** Comparison between classical (symbols) and quantum (lines) results for the Eley−Rideal reaction cross sections of Figure 2. From left to right for $v = 0$, 1, and 2, respectively.

the studied adiabatic model is better than the diabatic one in describing the dynamics even at low energies, as the product molecule forms early in the collision process and leaves the surface with sizable translational energy that the carbon atom hardly has time to relax. See the ample discussion on this point in the recent papers by Morisset et al.[22] and Bachellerie et al.[45] Note that in the first paper, a full quantum dynamical study including the effect of carbon relaxation has been performed at the expense of reducing the dynamics in the collinear configuration, whereas in the second one, a detailed dynamical model for the lattice has been introduced but calculations have been performed with classical means only.

**C. The Role of the Substrate Model.** A direct comparison between present and previous results from different groups is hard to perform as different researchers adopted different potential and/or dynamical models. Furthermore, the used potential energy surfaces are not always publicly available, and this prevents one from performing dynamical calculations under similar conditions. There are, however, global differences that become evident under simplified conditions and which might persist at any level of description. One of them is the behavior of the reaction probability in the collinear 2D approximation. Indeed, apart from the effect of the possible presence of a tiny barrier in the reaction profile, some PESs give rise to a sizable reaction probability and to a resonant behavior in the whole energy range 0−0.5 eV, whereas others (including the present ones) give rise to a smooth (almost free of resonances) decreasing probability as the energy decreases in the same range. Although neglected so far, this marked difference is more important than other subtler points (e.g., the motion of the carbon atom or the presence of a tiny barrier) in determining the global dynamical behavior of the system.

We therefore focus here on the results reported in refs 22 and 44 for the collinear case which, apart from an evident resonant structure, show quite large reaction probabilities. As the PES(s) used in refs 44 and 22 (and recently extended in ref 45) are not publicly available, we recomputed the relevant 2D cuts by employing similar electronic structure means, namely DFT with an atom-centered basis set, using coronene as a substrate model. Electronic structure calculations have been performed with the help of GAUSSIAN code[51] both for the adiabatic and diabatic models and fitted to the same functional form used by Sha et al.[28] Furthermore, plane-wave based DFT calculations of the same reaction have been performed using graphene as a model substrate and for different sizes of the unit cell, with similar parameters as used in our recent work.[20] Details of these calculations will be reported in a forthcoming paper, and here we limit ourselves to report the main results.

The potential energy surfaces computed with the above two substrate models at similar level of theory only qualitatively look

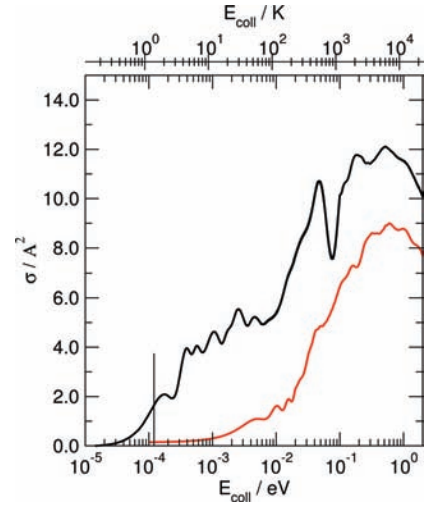


**Figure 6.** Eley−Rideal cross sections in the diabatic (red) and adiabatic (black) models for $v = 0$.

similar. Both of them show a simple downhill route from reagent to product, similar to the one reported in Figure 7, left panel, for the (diabatic) coronene substrate model, but the *shape* of the PES in the corner region is different for the two substrate models considered and for different level of theory. This is shown in Figure 7, right panel, where the different curves reported refer to the same cut in the entrance channel, namely with the target H atom fixed at its equilibrium position (in the absence of the second atom).

This seemingly small dependence of the PES features on the choice of the substrate model leads to significant differences in the computed reaction probabilities, as a consequence of purely classical effects. This is reasonable as the reaction lacks any bottleneck and is therefore sensitive to any other, usually less important features such as the shape of the corner. This is best seen in model calculations using the same modified London−Eyring−Polanyi−Sato (LEPS) functional form defined by Sha et al.[28] and varying one of the Sato parameter, while keeping all other parameters at their optimal values defined in ref 28. When changing the Sato parameter for the target H atom in the range 0.0−0.8, we smoothly modify the PES along the same lines as observed when going from graphene to coronene, without introducing any undesired artifact (see Figure 8, left panel). (The same is not true for negative values of this parameter as they lead to the appearance of a well in the exit channel). Correspondingly, the reaction probabilities drastically change, and show an almost uniform unit value at the higher end of the interval (Figure 8, center and right panels).

It is reasonable to expect that similar dependence on the substrate model has to be found in more realistic dynamical

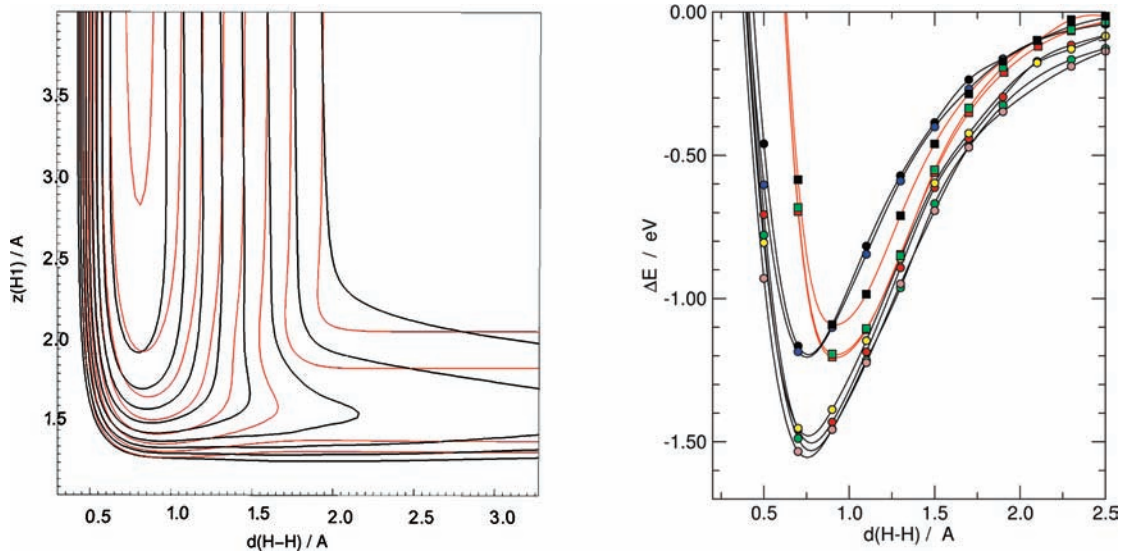


**Figure 7.** Results of *first principles* electronic structure calculations on the reaction energetics performed using different models for the surface. Left panel: contour lines (black) for the diabatic collinear PES computed at the DFT/PW91-VWN/cc-pVDZ level using coronene as a substrate model. Also shown as red lines is the diabatic PES of Sha et al.,[28] corresponding to a periodic graphitic model. Right panel: energy as a function of the projectile H atom height for fixed heights of both the target hydrogen and the underneath carbon atoms, in collinear geometry. Circles for the coronene model (black for B3LYP/cc-pVDZ, red for PB86/cc-pVDZ, green for PW91 VWN/cc-pVDZ, blue for B3LYP/cc-pVTZ, yellow for PB86/cc-pVTZ, brown for PW91 VWN/cc-pVTZ), squares for a periodic graphene model (plane-wave based DFT/PBE for a 2 × 2 cell in black, 3 × 3 in red, 4 × 4 in green).

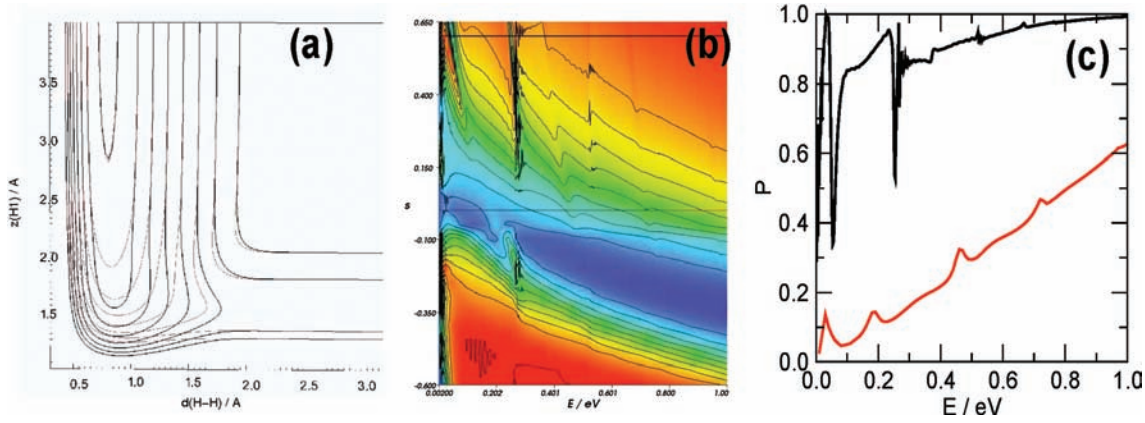


**Figure 8.** Results of model calculations in which the target-atom Sato parameter $s$ defined in the diabatic PES of Sha et al.[28] has been changed in the interval [−0.6, 0.7]. (a) Contour lines of the PESs with $s = 0.6$ (black) and $s = 0.035$ (red). (The latter value corresponds to that optimized in ref 28.) (b) Reaction probability as function of both the energy and $s$ ($x$ and $y$ axes, respectively). Horizontal lines mark the values $s = 0.60, 0.035$. (c) Reaction probability for $s = 0.60, 0.035$ (black and red line, respectively).

models, at least for near head-on collisions. The question then arises whether the coronene model (or similar models based on small polycyclic aromatic hydrocarbons) is realistic enough to describe Eley−Rideal hydrogen formation on graphite.

**D. Energy Barrier to Reaction?** It has been found that density functional theory calculations of the potential energy surface shows a tiny barrier (∼10 meV) in the reaction profile. As this value is too small for being accurately predicted by DFT techniques, we decided to neglect it by using the analytical PESs defined in ref 28. Its possible presence is currently hard to assess, for more accurate quantum chemistry techniques apply to cluster models only, but, according to the discussion above, these might not be realistic enough to describe hydrogen recombination on graphite. This is quite unpleasant as its influence on the low-energy dynamics would be enormous, as already emphasized by Morisset et al.[22,44] If this were the case, then our computed cross sections for the reaction involving chemisorbed species would be further reduced for energies below barrier by the corresponding tunneling probability and our main conclusion that Eley−Rideal reaction is more efficient if it involves physisorbed atoms would be enforced. The main point here is that this is true even when such a barrier is absent. Incidentally, we note here that analogous problems appear for other regions of the configuration space (e.g., the asymptotic region of the entrance channel) which too have a strong influence on the low energy dynamics. The result is that such exothermic surface reactions (the only ones possible in the extreme conditions of the ISM) present a challenge to theoreticians in that they require an accuracy on the potential energy surface (∼10 meV) which is currently impossible to attain.

**E. Energy Dissipation to the Substrate.** As already emphasized in Section II, we adopted here a rigid surface model, thereby completely neglecting the effect of energy dissipation to the lattice. This can be quite important, especially in determining how the reaction exothermicity is partitioned among the various molecular and surface degrees of freedom. However, similar to the point above, describing the lattice

dynamics at typical ISM conditions is a further challenge to theoreticians. It is not only a problem of building a reasonably accurate lattice potential, as energy dissipation occurs in such "deep" quantum regime where both the system (low energy H atoms) and the bath (a low temperature surface) hardly suit to common approximations. Much work has to be done to apply exact wavepacket techniques[32−35] or properly designed approximations (e.g., ref 35) to this problem. In this respect, the use of a time-dependent wavepacket approach which takes care of the special needs of a low energy dynamics, as the one outlined in Section II, can be considered an important step in this direction.

## IV. Summary

In this work, we have investigated quantum dynamically collision induced processes involving hydrogen atoms on graphite at cold collision energies typical of diffuse interstellar clouds. Both chemisorbed and physisorbed target species have been considered, and the Eley−Rideal reaction and trapping dynamics have been analyzed. Results have been obtained with the help of a time-dependent wavepacket method and represent—to the best of our knowledge—the lowest-energy results ever obtained with such an approach. This is promising for introducing in the near future the effects of energy dissipation to the lattice, and work is in progress along this direction. We further critically examined the approximations used to define the adopted dynamical model, and considered a number of issues which have not found proper consideration so far. Among these, the need of a quantum description in the astrophysically relevant collision energy range and the importance of the substrate model used to build the potential energy surface governing the reaction when chemisorbed species are involved.

Results show that chemisorbed and physisorbed H atoms behave differently at typical interstellar cloud conditions (see lower right panel in Figure 4). The first undergo a collinear-dominated reaction mechanism, which becomes increasingly inefficient when the energy decreases below $\sim 10^{-2}$ eV, probably because of the quantum reflection of the incident wavepacket from the strong, short-range potential characterizing the exit (reaction) channel. Under these conditions, trapping of the incident atom (not shown) is negligible, with cross sections vanishing in the same energy range. These dynamical results likely hold independently on the fact that the chemisorbed atom is an isolated one or is part of a cluster, thereby suggesting that the chemisorbed species play a minor role in hydrogen formation at interstellar cloud conditions, even when a barrierless chemisorption process occurs. In contrast, physisorbed species are weakly bound to the surface and may promptly release hydrogen molecules or form-trapped species even at low energies, with cross sections that are 2−3 times larger than the previous ones in the relevant energy range. As already mentioned in the Introduction, taking also into account the tight kinetic constraints in chemisorbing H atoms, we are tempted to conclude, based on present results, that hydrogen formation in diffuse clouds either involves physisorbed species only (and sufficiently low surface temperature to limit desorption) or cannot be explained by a simple graphitic model. There remain, however, several open questions concerning both the accuracy of the potential and the dynamics, and they represent challenging problems to theoreticians.

**Acknowledgment.** We dedicate this paper to Vincenzo Aquilanti whose achievements and successes in the field of chemical reaction dynamics have been a model for several researchers.

## References and Notes

(1) Gould, R. J.; Salpeter, E. E. *Astrophys. J.* **1963**, *138*, 393.
(2) Hollenbach, D.; Salpeter, E. E. *J. Chem. Phys.* **1970**, *53*, 79.
(3) Hollenbach, D.; Salpeter, E. E. *Astrophys. J.* **1971**, *163*, 155.
(4) Greenberg, J. M. *Surf. Sci.* **2002**, *500*, 793.
(5) Williams, D. A.; Herbst, E. *Surf. Sci.* **2002**, *500*, 823.
(6) Draine, B. T. *Annu. Rev. Astron. Astrophys.* **2003**, *41*, 241.
(7) Zecho, T.; Güttler, A.; Sha, X.; Jackson, B.; Küppers, J. *J. Chem. Phys.* **2002**, *117*, 8486.
(8) Güttler, A.; Zecho, T.; Küppers, J. *Surf. Sci.* **2004**, *570*, 218.
(9) Güttler, A.; Zecho, T.; Küppers, J. *Chem. Phys. Lett.* **2004**, *395*, 171.
(10) Zecho, T.; Güttler, A.; Küppers, J. *Carbon* **2004**, *42*, 609.
(11) Jeloaica, L.; Sidis, V. *Chem. Phys. Lett.* **1999**, *300*, 157.
(12) Sha, X.; Jackson, B. *Surf. Sci.* **2002**, *496*, 318.
(13) Kerwin, J.; Sha, X.; Jackson, B. *J. Phys. Chem. B* **2006**, *110*, 18811.
(14) Ferro, Y.; Marinelli, F.; Allouche, A. *Chem. Phys. Lett.* **2003**, *368*, 609.
(15) Kerwin, J.; Jackson, B. *J. Chem. Phys.* **2008**, *128*, 084702.
(16) Hornekær, L.; Šljivačanin, Ž.; Xu, W.; Otero, R.; Rauls, E.; Stensgaard, I.; Lægsgaard, E.; Hammer, B.; Besenbacher, F. *Phys. Rev. Lett.* **2006**, *96*, 156104.
(17) Hornekær, L.; Rauls, E.; Xu, W.; Šljivačanin, Ž.; Otero, R.; Stensgaard, I.; Løegsgaard, E.; Hammer, B.; Besenbacher, F. *Phys. Rev. Lett.* **2006**, *97*, 186102.
(18) Hornekær, L.; Xu, W.; Otero, R.; Zecho, T.; Lægsgaard, E.; Besenbacher, F. *Chem. Phys. Lett.* **2007**, *446*, 237.
(19) Andree, A.; Le Lay, M.; Zecho, T.; Küppers, J. *Chem. Phys. Lett.* **2006**, *425*, 99.
(20) Casolo, S.; Lovvik, O. M.; Martinazzo, R.; Tantardini, G. F. *J. Chem. Phys.* **2009**, *130*, 054704.
(21) Rougeau, N.; Teillet-Billy, D.; Sidis, V. *Chem. Phys. Lett.* **2006**, *431*, 135.
(22) Morisset, S.; Aguillon, F.; Sizun, M.; Sidis, V. *J. Chem. Phys.* **2004**, *121*, 6493.
(23) Morisset, S.; Aguillon, F.; Sizun, M.; Sidis, V. *J. Chem. Phys.* **2005**, *122*, 194702.
(24) Bachelleire, D.; Sizun, M.; Anguillon, F.; Sidis, V. *J. Phys. Chem. A* **2009**, *113*, 108.
(25) Bonfanti, M.; Martinazzo, R.; Tantardini, G. F.; Ponti, A. *J. Phys. Chem. C* **2007**, *111*, 5825.
(26) Persson, M.; Jackson, B. *J. Chem. Phys.* **1995**, *102*, 1078.
(27) Lemoine, D.; Jackson, B. *Comput. Phys. Commun.* **2001**, *137*, 415.
(28) Sha, X.; Jackson, B.; Lemoine, D. *J. Chem. Phys.* **2002**, *116*, 7158.
(29) Martinazzo, R.; Tantardini, G. F. *J. Phys. Chem. A* **2005**, *109*, 9379.
(30) Martinazzo, R.; Tantardini, G. F. *J. Chem. Phys.* **2006**, *124*, 124702.
(31) Martinazzo, R.; Tantardini, G. F. *J. Chem. Phys.* **2006**, *124*, 124703.
(32) Beck, M. H.; Jackle, A.; Worth, G. A.; Meyer, H.-D. *Phys. Rep.* **2000**, *324*, 1.
(33) Burghardt, I.; Nest, M.; Worth, G. A. *J. Chem. Phys.* **2003**, *119*, 5364.
(34) *Multidimensional Quantum Dynamics: MCTDH Theory and Application*; Meyer, H.-D.; Gatti, F.; Worth, G. A., Eds.; Wiley-VCH: New York, 2009.
(35) Martinazzo, R.; Nest, M.; Saalfrank, P.; Tantardini, G. F. *J. Chem. Phys.* **2006**, *125*, 194102.
(36) Manolopoulos, D. E. *J. Chem. Phys.* **2002**, *117*, 9552.
(37) Borisov, A. G. *J. Chem. Phys.* **2001**, *114*, 7770.
(38) Martinazzo, R.; Tantardini, G. F. *J. Chem. Phys.* **2005**, *122*, 094109.
(39) Messiah, A. *Quantum Mechanics*; Dover Publications: Mineola, NY, 1999; Ch. III.
(40) Jackson, B.; Lemoine, D. *J. Chem. Phys.* **2001**, *144*, 474.
(41) Meijer, A.; Farebrother, A.; Clary, D. *J. Phys. Chem. A* **2001**, *105*, 2173.
(42) Meijer, A.; Farebrother, A.; Clary, D. *J. Phys. Chem. A* **2002**, *106*, 8996.
(43) Meijer, A.; Fisher, A.; Clary, D. *J. Phys. Chem. A* **2003**, *107*, 10862.
(44) Morisset, S.; Aguillon, F.; Sizun, M.; Sidis, V. *Phys. Chem. Chem. Phys.* **2003**, *5*, 506.
(45) Bachellerie, D.; Sizun, M.; Anguillon, F.; Teillet-Billy, D.; Rougeau, N.; Sidis, V. *Phys. Chem. Chem. Phys.* **2009**, *11*, 2715.
(46) Rutigliano, M.; Cacciatore, M.; Billing, G. *Chem. Phys. Lett.* **2001**, *340*, 13.
(47) Rutigliano, M.; Cacciatore, M. *ChemPhysChem* **2008**, *9*, 171.
(48) Ko, Y.; Ree, J.; Kim, Y.; Shin, H. *Bull. Korean Chem. Soc.* **2002**, *23*, 1737.
(49) Ree, J.; Kim, Y.; Shin, H. *Chem. Phys. Lett.* **2002**, *353*, 368.
(50) Ree, J.; Kim, Y.; Shin, H. *Bull. Korean Chem. Soc.* **2007**, *28*, 635.
(51) Frisch, M. J.; Trucks, G. W.; Schlegel, H. B.; Scuseria, G. E.; Robb, M. A.; Cheeseman, J. R.; Zakrzewski, V. G.; Montgomery, J. A., Jr.; Stratmann,

R. E.; Burant, J. C.; Dapprich, S.; Millam, J. M.; Daniels, A. D.; Kudin, K. N.; Strain, M. C.; Farkas, O.; Tomasi, J.; Barone, V.; Cossi, M.; Cammi, R.; Mennucci, B.; Pomelli, C.; Adamo, C.; Clifford, S.; Ochterski, J.; Petersson, G. A.; Ayala, P. Y.; Cui, Q.; Morokuma, K.; Malick, D. K.; Rabuck, A. D.; Raghavachari, K.; Foresman, J. B.; Cioslowski, J.; Ortiz, J. V.; Stefanov, B. B.; Liu, G.; Liashenko, A.; Piskorz, P.; Komaromi, I.; Gomperts, R.; Martin, R. L.; Fox, D. J.; Keith, T.; Al-Laham, M. A.; Peng, C. Y.; Nanayakkara, A.; Gonzalez, C.; Challacombe, M.; Gill, P. M. W.; Johnson, B. G.; Chen, W.; Wong, M. W.; Andres, J. L.; Head-Gordon, M.; Replogle, E. S.; Pople, J. A. Gaussian 98, revision x.x; Gaussian, Inc.: Pittsburgh, PA, 1998. Frisch, M. J.; Trucks, G. W.; Schlegel, H. B.; Scuseria, G. E.; Robb, M. A.; Cheeseman, J. R.; Zakrzewski, V. G.; Montgomery, J. A., Jr; Stratmann, R. E.; Burant, J. C., et al., *Gaussian 98, Revision A.7*; Gaussian Inc.: Pittsburgh PA, 1998.

JP9040265